Contribution from the Faculty of Chemistry,
University of Bielefeld, D-4800 Bielefeld, West Germany

# Preparation and X-ray Crystal and Molecular Structure of $\{Mo_2S_8Ag_4\}(PPh_3)_4$, a Compound with a Metal–Sulfur Cage

A. MÜLLER,* H. BÖGGE, E. KÖNIGER-AHLBORN, and W. HELLMANN

*Received April 2, 1979*

$\{Mo_2S_8Ag_4\}(PPh_3)_4$ has been prepared by the extraction of an aqueous solution of $(NH_4)_2MoS_4$ with a solution of $(C_6H_5)_3P$ and $AgNO_3$ in $CH_2Cl_2$. The crystal and molecular structure of $\{Mo_2S_8Ag_4\}(PPh_3)_4$ was determined from single-crystal X-ray diffractometer data. The compound crystallizes in the triclinic space group $P\bar{1}$ with one molecule in the unit cell: $a$ = 12.246 (2), $b$ = 12.905 (2), $c$ = 13.211 (2) Å; $\alpha$ = 97.81 (1), $\beta$ = 113.31 (1), $\gamma$ = 91.52 (1)°; $V$ = 1892.1 Å$^3$; $d_{calcd}$ = 1.69 g cm$^{-3}$. Anisotropic (except for the C atoms) least-squares refinement resulted in a conventional final $R$ factor of 0.058 for 5183 independent data. The structure can be described as a cage (with a center of inversion), fused by two six-membered $SAg_2S_2Mo$ rings which are connected by metal–sulfur bonds. Mo (106.42 (10)–112.98 (9)°) and Ag (distorted, angles varying between 92.62 (8) and 129.08 (8)°) are tetrahedrally coordinated. $MoS_4^{2-}$ acts as a terdentate ligand.

## Introduction

Considerable interest has been shown in recent years concerning polynuclear transition-metal sulfur compounds.[1] Synthetic routes for compounds containing different metal atoms linked by sulfur are of special interest.[2] This type of compound can be generated by thiometalates like $MoS_4^{2-}$ or $WS_4^{2-}$.[3] Whereas complexes containing a transition element with an open shell (like the thio heteroanion $[Co(WS_4)_2]^{2-}$[4,5]) can be classified according to the rules of classical complex chemistry, unusual coordination is found in compounds containing metals with closed d shells, e.g., $[Sn_2(WS_4)_4]^{4-}$ (novel dimeric structure),[6] $WOS_3Cu_3Cl(PPh_3)_3$ (cubane type structure),[7] or $[Au_2(WS_4)_2]^{2-}$ (ring structure).[8]

In this paper the preparation and crystal structure of $\{Mo_2S_8Ag_4\}(PPh_3)_4$ (see Figure 1), a compound generated by $MoS_4^{2-}$ and containing a metal–sulfur cage fused by two connected six-membered $SAg_2S_2Mo$ rings, are reported.

## Experimental Section

$\{Mo_2S_8Ag_4\}(PPh_3)_4$ was prepared by the extraction of an aqueous solution (100 mL) of 0.16 g of $(NH_4)_2MoS_4$ with a solution of 0.73 g of $P(C_6H_5)_3$ and 0.21 g of $AgNO_3$ in 25 mL of $CH_2Cl_2$. Suitable crystals for the X-ray structure analysis were obtained by topping the organic phase with a mixture of acetone (10 mL) and *n*-pentane (50 mL) and keeping the two-phase system for 2–3 days. (Immediate precipitation with *n*-pentane yields 0.3 g of $\{Mo_2S_8Ag_4\}(PPh_3)_4$.) The compound, which is sparingly soluble in organic solvents such as $CH_2Cl_2$, acetone, and nitromethane, shows characteristic infrared absorptions at 515 (t, $\nu$(Mo–S)), 453, and 438 cm$^{-1}$ (br, $\nu$(Mo–S)). The infrared spectra (Nujol mull) were measured with a Perkin–Elmer Model 180 spectrophotometer.

## X-ray Structure Determination[9]

The molecular structure of $\{Mo_2S_8Ag_4\}(PPh_3)_4$ was determined from a single-crystal X-ray structure analysis. A summary of the crystal data and details concerning the intensity data collection is given in Table I. The unit cell parameters were obtained at 22 °C by a least-squares refinement of the angular settings of eight high-angle reflections. Intensity data were collected on a Syntex $P2_1$ four-circle diffractometer. No absorption correction had to be applied. The data were corrected for Lorentz and polarization effects.

The Mo and Ag atoms were located from a three-dimensional Patterson synthesis. The positional parameters of the remaining nonhydrogen atoms were deduced from successive difference-Fourier syntheses. Several cycles (with the carbon atoms being refined independently) converged at $R = \sum||F_o| - |F_c||/\sum|F_o| = 0.058$ and $R_w = [\sum w(|F_o| - |F_c|)^2/\sum w|F_o|^2]^{1/2} = 0.054$ ($1/w = \sigma^2(F_o)^2$).

**Table I.** Summary of Crystal Data and Intensity Data Collection for $\{Mo_2S_8Ag_4\}(PPh_3)_4$

| | | | |
|---|---|---|---|
| $a$, Å | 12.246 (2) | $F$(000), e | 952 |
| $b$, Å | 12.905 (2) | cryst system | triclinic |
| $c$, Å | 13.211 (2) | space group | $P\bar{1}$ |
| $\alpha$, deg | 97.81 (1) | cryst dimens, mm | 0.3 × 0.25 × 0.3 |
| $\beta$, deg | 113.31 (1) | abs coeff | 16.4 |
| $\gamma$, deg | 91.52 (1) | $\mu$(Mo K$\alpha$), cm$^{-1}$ | |
| $V$, Å$^3$ | 1892 | fw | 1929.0 |
| $d_{calcd}$, g cm$^{-3}$ | 1.69 | empirical formula | $C_{72}H_{60}Ag_4Mo_2P_4S_8$ |
| $Z$ | 1 | | |

| | |
|---|---|
| radiation | graphite-monochromated Mo K$\alpha$ ($\lambda$ 0.710 69 Å) |
| data collecn | $2\theta$–$\theta$ mode; $2\theta$ range 4–50°; scan from 1° below K$\alpha_1$ to 1° above K$\alpha_2$ in $2\theta$; scan speed 2.93–29.3°/min; bkgd scan time ratio 0.75; ref rflctn every 50 rflctns |
| no. of measd rflctns ($(\sin\theta)/\lambda < 0.59$ Å$^{-1}$) | 6697 |
| no. of obsd rflctns ($I \geq 1.96\,\sigma(I)$) | 5183 |
| no. of variables | 226 |

During the last cycles of refinement the temperature factors of all atoms (except for the carbon atoms) were treated in the anisotropic form. In the final stage of refinement, no parameter shifted more than 0.12$\sigma$, where $\sigma$ is the standard deviation of the parameter.

The atomic scattering factors for Mo, Ag, S, P, and C were taken from ref 10. Anomalous dispersion corrections were applied to the Mo, Ag, and S atoms. The final $\Delta F$ map contained no significant peaks. The final positional and thermal parameters are given in Table II. A list of observed and calculated structure factors is available.[11]

## Results and Discussion

The structure consists of one molecule, $\{Mo_2S_8Ag_4\}(PPh_3)_4$, per unit cell. The interatomic distances are given in Table III. Bond angles are collected in Table IV. The molecule has $\bar{1}$ symmetry according to the exact crystallographic $\bar{1}$ site symmetry (center of inversion at (0, $^1/_2$, 0)). Figure 2 shows the heavy-atom skeleton of the molecular structure, with a cage fused by two six-membered $SAg_2S_2Mo$ rings which are connected by nearly parallel Ag–S and Mo–S bonds, respectively. The molybdenum atoms are tetrahedrally coordinated (106.42 (10)–112.98 (9)°), whereby the angles between the terminal and the bridging Mo–S bonds are smaller

0020-1669/79/1318-2301$01.00/0 

**Table II.** Positional and Thermal (Å²)[a] Parameters for $\{Mo_2S_8Ag_4\}(PPh_3)_4$ with Standard Deviations

| atom | $x$ | $y$ | $z$ | $B_{11}$ | $B_{22}$ | $B_{33}$ | $B_{12}$ | $B_{13}$ | $B_{23}$ |
|---|---|---|---|---|---|---|---|---|---|
| Mo | 0.0345 (1) | 0.3648 (1) | 0.1201 (1) | 2.75 (3) | 2.63 (3) | 2.74 (3) | 0.35 (2) | 0.90 (3) | 0.79 (2) |
| S1 | −0.0560 (2) | 0.4872 (2) | 0.1873 (2) | 3.42 (10) | 3.29 (10) | 4.30 (11) | 0.47 (8) | 2.03 (9) | 0.82 (8) |
| S2 | −0.0818 (2) | 0.2994 (2) | −0.0542 (2) | 3.04 (10) | 3.81 (11) | 3.28 (10) | −0.29 (8) | 0.88 (8) | 0.62 (8) |
| S3 | 0.2174 (2) | 0.4238 (2) | 0.1414 (2) | 2.72 (10) | 4.45 (11) | 3.42 (10) | 0.21 (9) | 0.90 (8) | 0.05 (9) |
| S4 | 0.0547 (3) | 0.2423 (2) | 0.2150 (2) | 6.47 (16) | 4.44 (13) | 5.13 (14) | 1.27 (12) | 2.02 (12) | 2.27 (11) |
| Ag1 | 0.1144 (1) | 0.3604 (1) | −0.0675 (1) | 3.39 (3) | 4.72 (4) | 3.75 (3) | 0.55 (3) | 1.59 (3) | 0.28 (3) |
| Ag2 | 0.1447 (1) | 0.5799 (1) | 0.2242 (1) | 3.50 (3) | 3.39 (3) | 4.63 (4) | −0.23 (3) | 0.81 (3) | −0.21 (3) |
| P1 | 0.2354 (2) | 0.2398 (2) | −0.1269 (1) | 3.17 (11) | 3.77 (11) | 3.82 (11) | 0.69 (9) | 1.56 (9) | 0.95 (9) |
| P2 | 0.2750 (2) | 0.7009 (2) | 0.3852 (2) | 3.16 (10) | 3.05 (10) | 3.19 (10) | 0.16 (8) | 0.81 (9) | 0.41 (8) |

| atom | $x$ | $y$ | $z$ | $B$, Å² | atom | $x$ | $y$ | $z$ | $B$, Å² |
|---|---|---|---|---|---|---|---|---|---|
| C1 | 0.2431 (8) | 0.1158 (7) | −0.0728 (7) | 4.2 (2) | C19 | 0.4306 (8) | 0.6677 (7) | 0.4439 (7) | 3.7 (1) |
| C2 | 0.1443 (8) | 0.0747 (8) | −0.0604 (8) | 5.2 (2) | C20 | 0.4688 (9) | 0.6062 (8) | 0.3720 (8) | 5.5 (2) |
| C3 | 0.1459 (10) | −0.0226 (9) | −0.0237 (9) | 6.3 (3) | C21 | 0.5938 (11) | 0.5808 (9) | 0.4179 (10) | 7.1 (3) |
| C4 | 0.2422 (10) | −0.0768 (9) | 0.0015 (9) | 6.6 (3) | C22 | 0.6651 (10) | 0.6192 (9) | 0.5294 (9) | 6.6 (3) |
| C5 | 0.3379 (12) | −0.0455 (11) | −0.0220 (12) | 9.2 (4) | C23 | 0.6220 (10) | 0.6748 (9) | 0.5948 (9) | 6.5 (3) |
| C6 | 0.3383 (11) | 0.0564 (11) | −0.0567 (11) | 8.1 (3) | C24 | 0.5020 (10) | 0.7026 (8) | 0.5566 (9) | 5.6 (2) |
| C7 | 0.1835 (8) | 0.2037 (7) | −0.2768 (8) | 4.6 (2) | C25 | 0.2334 (9) | 0.7136 (7) | 0.5050 (8) | 4.8 (2) |
| C8 | 0.1423 (10) | 0.2784 (8) | −0.3449 (9) | 5.9 (3) | C26 | 0.1794 (9) | 0.6217 (8) | 0.5180 (8) | 5.4 (2) |
| C9 | 0.1021 (11) | 0.2540 (9) | −0.4605 (10) | 7.3 (3) | C27 | 0.1576 (11) | 0.6249 (9) | 0.6164 (10) | 7.1 (3) |
| C10 | 0.1089 (14) | 0.1604 (12) | −0.5069 (13) | 10.8 (5) | C28 | 0.1882 (11) | 0.7116 (10) | 0.6928 (10) | 7.6 (3) |
| C11 | 0.1290 (20) | 0.0752 (17) | −0.4461 (18) | 17.0 (7) | C29 | 0.2363 (11) | 0.8030 (10) | 0.6796 (10) | 7.4 (3) |
| C12 | 0.1828 (16) | 0.1011 (13) | −0.3239 (14) | 12.2 (5) | C30 | 0.2630 (10) | 0.8050 (9) | 0.5814 (9) | 6.3 (3) |
| C13 | 0.3904 (8) | 0.2889 (7) | −0.0798 (7) | 4.2 (2) | C31 | 0.2821 (8) | 0.8346 (7) | 0.3558 (7) | 4.0 (2) |
| C14 | 0.4520 (10) | 0.2719 (9) | −0.1486 (9) | 6.3 (3) | C32 | 0.1746 (9) | 0.8789 (7) | 0.3139 (8) | 4.7 (2) |
| C15 | 0.5761 (11) | 0.3095 (9) | −0.1051 (10) | 7.4 (3) | C33 | 0.1751 (10) | 0.9800 (9) | 0.2838 (9) | 6.5 (3) |
| C16 | 0.6248 (11) | 0.3667 (9) | −0.0059 (10) | 7.3 (3) | C34 | 0.2781 (11) | 1.0299 (9) | 0.2946 (10) | 7.2 (3) |
| C17 | 0.5743 (13) | 0.3825 (11) | 0.0677 (12) | 9.7 (4) | C35 | 0.3873 (12) | 0.9864 (10) | 0.3342 (10) | 7.9 (3) |
| C18 | 0.4462 (11) | 0.3436 (10) | 0.0249 (10) | 7.6 (3) | C36 | 0.3909 (10 | 0.8830 (8) | 0.3675 (9) | 6.2 (3) |

[a] The anisotropic temperature factor used is defined as $\exp[-1/4(B_{11}h^2a^{*2} + B_{22}k^2b^{*2} + B_{33}l^2c^{*2} + 2B_{12}hka^*b^* + 2B_{13}hla^*c^* + 2B_{23}klb^*c^*)]$.

**Table III.** Interatomic Distances (Å) in $\{Mo_2S_8Ag_4\}(PPh_3)_4$ with Standard Deviations[a]

| | | | |
|---|---|---|---|
| | A. Mo-S, Ag-S, and Ag-P Distances | | |
| Mo-S1 | 2.235 (3) | Ag1-S3 | 2.540 (2) |
| Mo-S2 | 2.204 (2) | Ag1-P1 | 2.438 (3) |
| Mo-S3 | 2.243 (3) | Ag2-S1 | 2.538 (3) |
| Mo-S4 | 2.108 (3) | Ag2-S2a | 2.777 (2) |
| Ag1-S1a[a] | 2.629 (2) | Ag2-S3 | 2.513 (3) |
| Ag1-S2 | 2.587 (3) | Ag2-P2 | 2.406 (2) |
| | B. Molybdenum-Silver Distances | | |
| Mo···Ag1 | 2.998 (1) | Mo···Ag2 | 2.952 (1) |
| | C. Sulfur-Sulfur Distances | | |
| S1···S2 | 3.635 (3) | S2···S3 | 3.707 (3) |
| S1···S3 | 3.722 (4) | S2···S4 | 3.472 (3) |
| S1···S4 | 3.479 (4) | S3···S4 | 3.508 (4) |
| | D. Phosphorus-Carbon Distances | | |
| P1-C1 | 1.830 (9) | P2-C19 | 1.839 (10) |
| P1-C7 | 1.812 (10) | P2-C25 | 1.834 (10) |
| P1-C13 | 1.812 (11) | P2-C31 | 1.826 (9) |
| | E. Carbon-Carbon Distances | | |
| C1-C2 | 1.384 (16) | C19-C20 | 1.384 (14) |
| C2-C3 | 1.404 (15) | C20-C21 | 1.472 (18) |
| C3-C4 | 1.336 (18) | C21-C22 | 1.392 (16) |
| C4-C5 | 1.389 (21) | C22-C23 | 1.324 (17) |
| C5-C6 | 1.451 (19) | C23-C24 | 1.426 (18) |
| C6-C1 | 1.374 (18) | C24-C19 | 1.398 (13) |
| C7-C8 | 1.376 (14) | C25-C26 | 1.406 (15) |
| C8-C9 | 1.393 (16) | C26-C27 | 1.422 (17) |
| C9-C10 | 1.298 (20) | C27-C28 | 1.337 (17) |
| C10-C11 | 1.419 (27) | C28-C29 | 1.367 (18) |
| C11-C12 | 1.466 (27) | C29-C30 | 1.461 (17) |
| C12-C7 | 1.383 (20) | C30-C25 | 1.382 (15) |
| C13-C14 | 1.393 (16) | C31-C32 | 1.384 (15) |
| C14-C15 | 1.439 (19) | C32-C33 | 1.415 (15) |
| C15-C16 | 1.308 (17) | C33-C34 | 1.347 (19) |
| C16-C17 | 1.341 (21) | C34-C35 | 1.394 (20) |
| C17-C18 | 1.486 (22) | C35-C36 | 1.457 (17) |
| C18-C13 | 1.356 (15) | C36-C31 | 1.399 (16) |

[a] The index a refers to the transformation $\bar{x}, \bar{y}, \bar{z}$.

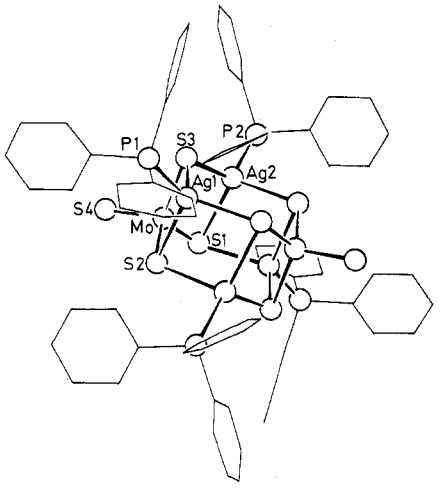


**Figure 1.** Stereochemistry of the $\{Mo_2S_8Ag_4\}(PPh_3)_4$ molecule.

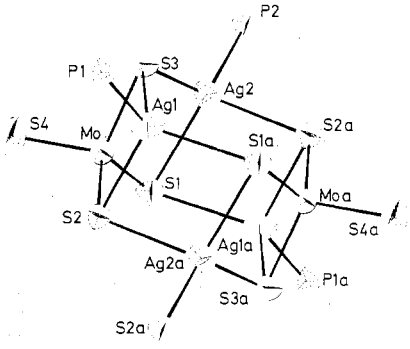


**Figure 2.** Heavy-atom skeleton of $\{Mo_2S_8Ag_4\}(PPh_3)_4$ (ORTEP diagram; 50% atomic vibration ellipsoids). The index a refers to the transformation $\bar{x}, \bar{y}, \bar{z}$.

than the angles between the bridging bonds. The terminal Mo–S bond (2.108 (3) Å) in the terdentate $MoS_4^{2-}$ ligand is significantly shorter than the bridging Mo–S bonds (2.204 (2)–2.243 (3) Å). The coordination polyhedron of Ag is a

**Table IV.** Bond Angles (deg) in $\{Mo_2S_8Ag_4\}(PPh_3)_4$ with Standard Deviations[a]

| | | | |
|---|---|---|---|
| A. Angles within $Mo_2S_8Ag_4P_4$ Cage | | | |
| S1-Mo-S2 | 109.93 (9) | S1-Ag2-S2a[a] | 101.42 (8) |
| S1-Mo-S3 | 112.46 (9) | S1-Ag2-S3 | 94.94 (8) |
| S1-Mo-S4 | 106.42 (10) | S1-Ag2-P2 | 129.08 (8) |
| S2-Mo-S3 | 112.98 (9) | S2a-Ag2-S3 | 101.32 (8) |
| S2-Mo-S4 | 107.24 (10) | S2a-Ag2-P2 | 103.06 (8) |
| S3-Mo-S4 | 107.44 (10) | S3-Ag2-P2 | 122.51 (8) |
| S1a-Ag1-S2 | 104.22 (8) | Mo-S1-Ag1a | 112.44 (10) |
| S1a-Ag1-S3 | 113.84 (8) | Mo-S1-Ag2 | 76.10 (8) |
| S1a-Ag1-P1 | 112.03 (8) | Ag1a-S1-Ag2 | 76.80 (7) |
| S2-Ag1-S3 | 92.62 (8) | Mo-S2-Ag1 | 77.03 (7) |
| S2-Ag1-P1 | 123.03 (8) | Mo-S2-Ag2a | 122.15 (10) |
| S3-Ag1-P1 | 109.87 (8) | Ag1-S2-Ag2a | 73.43 (6) |
| | | Mo-S3-Ag1 | 77.36 (8) |
| | | Mo-S3-Ag2 | 76.50 (8) |
| | | Ag1-S3-Ag2 | 118.50 (10) |
| B. Silver-Phosphorus-Carbon Angles | | | |
| Ag1-P1-C1 | 112.76 (32) | Ag2-P2-C19 | 114.36 (30) |
| Ag1-P1-C7 | 114.41 (34) | Ag2-P2-C25 | 115.05 (34) |
| Ag1-P1-C13 | 114.30 (32) | Ag2-P2-C31 | 112.61 (31) |
| C. Carbon-Phosphorus-Carbon Angles | | | |
| C1-P1-C7 | 105.50 (45) | C19-P2-C25 | 103.52 (44) |
| C1-P1-C13 | 103.93 (44) | C19-P2-C31 | 105.54 (42) |
| C7-P1-C13 | 104.92 (45) | C25-P2-C31 | 104.69 (45) |
| D. Phosphorus-Carbon-Carbon Angles | | | |
| P1-C1-C2 | 118.9 (8) | P2-C19-C20 | 116.7 (7) |
| P1-C1-C6 | 121.7 (8) | P2-C19-C24 | 119.4 (7) |
| P1-C7-C8 | 119.9 (8) | P2-C25-C26 | 115.3 (6) |
| P1-C7-C12 | 120.6 (10) | P2-C25-C30 | 121.4 (8) |
| P1-C13-C14 | 121.5 (8) | P2-C31-C32 | 116.4 (7) |
| P1-C13-C18 | 118.5 (8) | P2-C31-C36 | 119.8 (8) |
| E. Internal Angles of the Phenyl Rings | | | |
| C6-C1-C2 | 118.9 (10) | C24-C19-C20 | 123.9 (9) |
| C1-C2-C3 | 120.1 (9) | C19-C20-C21 | 117.0 (9) |
| C2-C3-C4 | 121.3 (11) | C20-C21-C22 | 118.5 (11) |
| C3-C4-C5 | 120.7 (12) | C21-C22-C23 | 121.6 (12) |
| C4-C5-C6 | 117.6 (13) | C22-C23-C24 | 123.3 (11) |
| C5-C6-C1 | 120.5 (12) | C23-C24-C19 | 115.7 (10) |
| C12-C7-C8 | 119.5 (12) | C30-C25-C26 | 123.0 (10) |
| C7-C8-C9 | 121.8 (11) | C25-C26-C27 | 117.1 (10) |
| C8-C9-C10 | 120.3 (13) | C26-C27-C28 | 120.9 (12) |
| C9-C10-C11 | 120.7 (17) | C27-C28-C29 | 122.8 (13) |
| C10-C11-C12 | 117.0 (19) | C28-C29-C30 | 119.1 (11) |
| C11-C12-C7 | 117.8 (16) | C29-C30-C25 | 116.9 (11) |
| C18-C13-C14 | 120.0 (10) | C36-C31-C32 | 123.6 (9) |
| C13-C14-C15 | 118.9 (11) | C31-C32-C33 | 118.3 (10) |
| C14-C15-C16 | 119.0 (12) | C32-C33-C34 | 120.1 (11) |
| C15-C16-C17 | 125.7 (13) | C33-C34-C35 | 123.1 (12) |
| C16-C17-C18 | 115.6 (13) | C34-C35-C36 | 118.6 (12) |
| C17-C18-C13 | 120.1 (12) | C35-C36-C31 | 116.4 (10) |

[a] The index a refers to the transformation $\bar{x}, \bar{y}, \bar{z}$.

distorted tetrahedron (92.62 (8)–129.08 (8)°), the terminal position being occupied by the triphenylphosphine ligand.

The bond lengths and angles in the $P(C_6H_5)_3$ ligand are, within the limit of error, in close agreement with literature data.[12] The average P–C distance (1.826 Å) and C–C bond length of 1.394 Å compare with mean values such as 1.821 and 1.373 Å in triphenylphosphine complexes.[12] There is also no significant deviation from planarity observable in the phenyl rings (see Table V).

As ions like $MoS_4^{2-}$ and $WS_4^{2-}$ can act as bi-, ter-, and tetradentate ligands in forming interesting polynuclear transition-metal compounds, it is worthwhile discussing the dependence of the metal–sulfur bond length on the type of coordination. In Table VI the bond distances in the free ions have been compared with those observed for the terminal and chelating bonds in polynuclear compounds. (All regularities are valid for molybdenum as well as tungsten compounds, as the corresponding bond distances are very similar.)

**Table V.** Weighted Least-Squares Planes within the $\{Mo_2S_8Ag_4\}(PPh_3)_4$ Molecule[a,b]

| atom | dev, Å | atom | dev, Å |
|---|---|---|---|
| Plane I: $0.0163X + 0.3102Y + 0.9505Z + 0.2961 = 0$ | | | |
| C1* | −0.029 | C5* | 0.054 |
| C2* | 0.023 | C6* | 0.017 |
| C3* | 0.018 | P1 | 0.056 |
| C4* | −0.053 | | |
| Plane II: $0.9797X + 0.1856Y + 0.0760Z - 3.8717 = 0$ | | | |
| C7* | −0.015 | C11* | 0.130 |
| C8* | 0.015 | C12* | −0.010 |
| C9* | 0.019 | P1 | −0.027 |
| C10* | −0.083 | | |
| Plane III: $0.1798X - 0.9189Y + 0.3512Z + 2.9839 = 0$ | | | |
| C13* | 0.001 | C17* | −0.032 |
| C14* | 0.010 | C18* | 0.002 |
| C15* | −0.034 | P1 | −0.005 |
| C16* | 0.040 | | |
| Plane IV: $0.3927X + 0.8849Y - 0.2504Z - 6.5878 = 0$ | | | |
| C19* | 0.013 | C23* | −0.006 |
| C20* | −0.011 | C24* | −0.011 |
| C21* | −0.006 | P2 | 0.037 |
| C22* | 0.015 | | |
| Plane V: $0.7907X - 0.3806Y + 0.4795Z + 0.2601 = 0$ | | | |
| C25* | −0.008 | C29* | 0.018 |
| C26* | 0.008 | C30* | −0.001 |
| C27* | 0.005 | P2 | −0.195 |
| C28* | −0.021 | | |
| Plane VI: $0.2435X - 0.2772Y - 0.9294Z + 6.4295 = 0$ | | | |
| C31* | −0.007 | C35* | 0.008 |
| C32* | 0.008 | C36* | 0.002 |
| C33* | −0.003 | P2 | 0.113 |
| C34* | −0.007 | | |

[a] The calculation was performed by using the program PLANE from the Syntex XTL program package. [b] Coordinates of atoms marked with asterisks were used to define the planes.

**Table VI.** Average Metal–Sulfur Bond Distances (Å) in Thiometalate Complexes

| $WS_4^{2-}$ ion | all bonds | ref | $MoS_4^{2-}$ ion | all bonds | ref |
|---|---|---|---|---|---|
| in $Cs_2WS_4$ | 2.189 | 13 | in $Cs_2MoS_4$ | 2.182 | 13 |
| in $(NH_4)_2WS_4$ | 2.177 | 13 | in $(GuH)_2MoS_4$[a] | 2.186 | 13 |
| in $(NH_4)_2WS_4$ | 2.165 | 14 | in $(NH_4)_2MoS_4$ | 2.178 | 15 |

| compd | coordination | chelating | terminal | all bonds | ref |
|---|---|---|---|---|---|
| $[Co(WS_4)_2]^{2-}$ | bidentate | 2.219 | 2.139 | 2.179 | 5 |
| $[Zn(WS_4)_2]^{2-}$ | bidentate | 2.233 | 2.156 | 2.195 | 16 |
| $[Au_2(WS_4)_2]^{2-}$ | bidentate | 2.243 | 2.136 | 2.190 | 8 |
| $[Ni(MoS_4)_2]^{2-}$ | bidentate | 2.227 | 2.151 | 2.189 | 17 |
| $[Sn_2(WS_4)_4]^{4-}$ | bidentate | 2.231 | 2.154 | 2.193 | 6 |
| $\{W_2S_8Ag_4\}(PPh_3)_4$ | terdentate | 2.234 | 2.121 | 2.206 | 18 |
| $\{Mo_2S_8Ag_4\}(PPh_3)_4$ | terdentate | 2.227 | 2.108 | 2.198 | this work |
| $(PPh_3)_3Ag_2WS_4$ | tetradentate | 2.206 | | 2.206 | 19 |
| $(Ph_2PCH_3)_2Au_2WS_4$ | tetradentate | 2.219 | | 2.219 | 20 |

[a] Gu stands for guanidine.

As expected, the terminal bonds in the $MoS_4$ and $WS_4$ tetrahedra are shorter than those in the chelating ones, whereby the average bond distances are in good agreement with those of the free ions (see Table VI). The terminal bond of a terdentate thiometalate ligand is shorter than that of a bidentate ligand, as in the former the predominant $\pi$-electron density is located in *one bond* only.

Whereas thiometalate complexes like $[Co(WS_4)_2]^{2-}$,[5] containing a transition element with an open d shell as central

atom, can be classified from the structural point of view according to the rules of classical complex chemistry, interesting transition-metal ring and cage systems are found in compounds containing metals with closed d shells. Especially remarkable are compounds with $Cu^+$ and $Ag^+$ (being very soft acids and having a high tendency to form metal–sulfur bonds), toward which $MoS_4^{2-}$ and $WS_4^{2-}$ act preferably as terdentate or tetradentate ligands.

**Acknowledgment.** We thank M. Dartmann for her assistance and the Deutsche Forschungsgemeinschaft, the Fonds der Chemischen Industrie, and the Minister für Wissenschaft und Forschung des Landes Nordrhein-Westfalen for financial support.

**Registry No.** $\{Mo_2S_8Ag_4\}(PPh_3)_4$, 70368-92-2; $(NH_4)_2MoS_4$, 15060-55-6.

**Supplementary Material Available:** Listing of structure factor amplitudes (18 pages). Ordering information is given on any current masthead page.

## References and Notes

(1) H. Vahrenkamp, *Angew. Chem., Int. Ed. Engl.*, **14**, 322 (1975).
(2) T. E. Wolff, J. M. Berg, C. Warrick, K. O. Hodgson, R. H. Holm, and R. B. Frankel, *J. Am. Chem. Soc.*, **100**, 4630 (1978); G. Christou, C. D. Garner, and F. E. Mabbs, *J. Chem. Soc., Chem. Commun.*, 740 (1978).
(3) E. Diemann and A. Müller, *Coord. Chem. Rev.*, **10**, 79 (1973).
(4) A. Müller and S. Sarkar, *Angew. Chem., Int. Ed. Engl.*, **16**, 705 (1977).
(5) A. Müller, N. Mohan, and H. Bögge, *Z. Naturforsch., B*, **33**, 978 (1978).
(6) A. Müller, I. Paulat-Böschen, B. Krebs, and H. Dornfeld, *Angew. Chem., Int. Ed. Engl.*, **15**, 633 (1976).
(7) A. Müller, T. K. Hwang, and H. Bögge, *Angew. Chem.*, in press.
(8) A. Müller, H. Dornfeld, G. Henkel, B. Krebs, and M. P. Viegers, *Angew. Chem., Int. Ed. Engl.*, **17**, 52 (1978).
(9) All computations were performed by using programs from the Syntex XTL structure-determination package.
(10) "International Tables for X-ray Crystallography", Vol. IV, Kynoch Press, Birmingham, England, 1974.
(11) Supplementary material.
(12) M. R. Churchill and K. L. Kalra, *Inorg. Chem.*, **13**, 1065 (1974).
(13) A. Müller, N. Mohan, and M. Dartmann, to be submitted for publication.
(14) K. Sasvari, *Acta Crystallogr.*, **16**, 719 (1963).
(15) J. Lapasset, N. Chezeau, and P. Belougne, *Acta Crystallogr., Sect. B*, **32**, 3087 (1976).
(16) I. Paulat-Böschen, B. Krebs, A. Müller, E. Königer-Ahlborn, H. Dornfeld, and H. Schulz, *Inorg. Chem.*, **17**, 1440 (1978).
(17) I. Søtofte, *Acta Chem. Scand., Ser. A*, **30**, 157 (1976).
(18) A. Müller, H. Bögge, and E. Königer-Ahlborn, *J. Chem. Soc., Chem. Commun.*, 739 (1978).
(19) A. Müller, H. Bögge, and E. Königer-Ahlborn, to be submitted for publication.
(20) J. C. Huffman, R. S. Roth, and A. R. Siedle, *J. Am. Chem. Soc.*, **98**, 4340 (1976).

# Notes

Contribution from the Department of Chemistry, Syracuse University, Syracuse, New York 13210

## Electrochemical Investigations of Some Azo Macrocyclic Ligands and Their Nickel(II) Complexes

James C. Dabrowiak,* Diane P. Fisher, Francis C. McElroy, and Daniel J. Macero

*Received December 21, 1978*

### Introduction

The redox properties of transition-metal complexes containing synthetic macrocyclic ligands have been actively investigated.[1-9] Unlike the porphyrins, synthetic cyclic structures, especially those based on a Schiff-base reaction, offer a wide assortment of macrocyclic ring sizes, with a variety of types and degrees of unsaturation. These features, combined with the fact that macrocyclic complexes are generally more resistant toward demetallation than are their acyclic counterparts, make this class of compounds useful agents for exploring the relationship between ligand structure and metal oxidation state. Redox transformations which are necessary to explore this relationship do not normally lead to complex decomposition. We reported earlier[8] on a series of Mn(III) complexes containing the macrocyclic Schiff base **1**. Electrochemical oxidation of compounds having stoichiometry

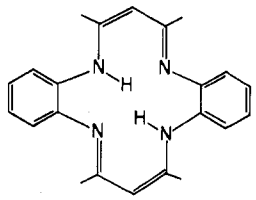

**1**

$Mn^{III}$–**1**(X), where X is $Cl^-$, $Br^-$, $SCN^-$, and $N_3^-$, did not lead to Mn(IV) complexes but lead instead to cation radicals containing an oxidized form of the ligand. Ligand oxidation also occurs if the bound metal ion is Ni(II), but in this case the cation radical which is formed rapidly dimerizes to form a dinuclear macrocyclic complex.[9] The dimer contains two macrocyclic units which are joined via the $\gamma$ position of the diiminate framework. Although ligand oxidation has been observed for other tetraaza diiminate frameworks,[3,4] at least one group of diiminate compounds similar in structure to **1** sustain a metal-centered oxidation in preference to a ligand oxidation.[1,5] In an attempt to more clearly define the various factors which influence the site at which a redox process will take place within this type of macrocyclic structure, we have examined the electrochemical properties of the two methine-substituted macrocyclic ligands **2** and **3** and their nickel complexes $Ni^{II}$–**2** and $Ni^{II}$–**3**.[10] Since the latter two compounds contain three distinct groups, which are potentially polarographically active, the metal ion, the macrocyclic ligand, and the azo chromophore, we have also investigated the electro-

0020-1669/79/1318-2304$01.00/0 